ELSEVIER

Journal of Alloys and Compounds 362 (2004) 143–150

Journal of ALLOYS AND COMPOUNDS

www.elsevier.com/locate/jallcom

Resonant soft X-ray emission spectroscopy of doped and undoped vanadium oxides

T. Schmitt [a,*], L.-C. Duda [a,*], M. Matsubara [b], A. Augustsson [a], F. Trif [c], J.-H. Guo [d], L. Gridneva [e], T. Uozumi [f], A. Kotani [b], J. Nordgren [a]

[a] *Department of Physics, Uppsala University, Ångström Laboratory, Box 530, S-75121 Uppsala, Sweden*
[b] *Institute for Solid State Physics, The University of Tokyo, 5-1-5 Kashiwanoha, Kashiwa-shi, Chiba 277-8581, Japan*
[c] *Department of Chemical Physics, Lund University, P.O. Box 124, S-22100 Lund, Sweden*
[d] *Advanced Light Source, Lawrence Berkeley National Laboratory, MS 7-222, One Cyclotron Road, Berkeley, CA 94720, USA*
[e] *MAX-lab National Laboratory, Lund University, Box 118, S-22100 Lund, Sweden*
[f] *College of Engineering, Osaka Prefecture University, Sakai, Osaka, 599-8531, Japan*

Received 15 September 2002; received in revised form 5 February 2003; accepted 10 February 2003

Abstract

Resonant soft X-ray emission (RSXE) spectra of NaV_2O_5, $Mo_xV_{1-x}O_2$ and V_2O_3 have been recorded for a series of excitation energies at resonances of the V L- and O K-absorption band. Resonant excitation allows us, firstly, to separate V 3d and O 2p projected density-of-states of the valence band and, secondly, to study charge-neutral low-energy excitations due to resonant inelastic X-ray scattering (RIXS). We found that both the V L- and the O K-emission spectra clearly show components originating from O 2p- and V 3d-states, reflecting the high degree of hybridization of the valence band in all compounds. At threshold excitation we observed that NaV_2O_5 spectra are dominated by RIXS whereas $Mo_xV_{1-x}O_2$ and V_2O_3 spectra show bandlike features, which may be due to differences in the correlation effects of the compounds. We compared the RSXE spectra with cluster model calculations, which gives a good account for NaV_2O_5 whereas the RSXE spectra of the other compounds show RIXS only at certain energies well above the threshold. In fact, we interpret the trend in the RSXE spectra of the $Mo_xV_{1-x}O_2$ compound system as a successive filling of the (rigid) V 3d band with increasing Mo content.
© 2003 Elsevier B.V. All rights reserved.

Keywords: Synchrotron radiation (E); X-Ray spectroscopies (E); Crystal and ligand fields (D); Localized electronic states (D); Electronic band structure (D)

1. Introduction

Transition metal oxides display a broad variety of electronic, magnetic and structural material properties. Vanadium oxides comprise a particularly interesting subgroup of the 3d transition metal compound family because many of them show metal-to-insulator transitions (MIT) [1] and other interesting phase transitions. V_2O_3 and VO_2 exhibit a MIT at 160 K [2] and 340 K [3], respectively. Metallic monoclinic MoO_2 is isostructural to the low temperature semiconducting phase of VO_2. By doping VO_2 with Mo the MIT temperature for the $Mo_xV_{1-x}O_2$ compound system can be shifted towards lower temperatures [4]. The insulator NaV_2O_5 has a charge ordering or spin-Peierls-like phase transition at 34 K [5]. In order to understand the underlying mechanisms for the various phase transitions displayed by these vanadium oxides it is essential to obtain a better understanding of their electronic structure at room temperature.

NaV_2O_5 possesses an orthorhombic crystal structure at room temperature and is centro-symmetric (P_{mmn}) with only one distinct V ion in a mixed valence state (average valence $V^{+4.5}$) [6]. The spins are carried by V–O–V molecular orbitals, the basic building blocks of the electronic structure of this unconventional spin-Peierls material. The electronic structure of insulating NaV_2O_5 has been widely studied by experimental and theoretical investigations [6–15]. By comparing model calculations of the electronic structure with experimental spectra gained from conventional optical techniques [7–11] the key parameters of the electronic structure can be determined. The room temperature insulating state of NaV_2O_5 has been theoretically investigated by band structure calculations within the framework of the local

* Corresponding authors.
E-mail addresses: thorsten.schmitt@fysik.uu.se (T. Schmitt), laurent.duda@fysik.uu.se (L.-C. Duda).

0925-8388/$ – see front matter © 2003 Elsevier B.V. All rights reserved.
doi:10.1016/S0925-8388(03)00575-9

density approximation without (LDA) [8,12–14] and with (LDA + U) [12–15] on-site Coulomb correlation U correction. By including the U correction the insulating character of NaV_2O_5 is explained. This visualizes the strongly correlated nature of its electronic structure. As a key feature, the V $3d_{xy}$ band is split into an upper and lower Hubbard subband opening a gap around the Fermi level between them [13].

At 160 K, V_2O_3 undergoes a MIT from the paramagnetic metal phase to the anti-ferromagnetic semiconducting phase [16,17]. This MIT is accompanied by a structural phase transition from the trigonal (corundum) structure in the metallic state to a monoclinic crystal structure in the semiconducting state [17]. As basic building blocks the metallic room temperature phase consists of distorted O_6-octahedra of which two-thirds are occupied by a V atom. The prime mechanism for the MIT is generally believed to be dominated by electron correlation effects [18,19]. However, the detailed origin of the MIT in V_2O_3 is still under debate and therefore experimental studies of the electronic structure are highly desirable.

Vanadium dioxide VO_2 undergoes a MIT from a paramagnetic metal with tetragonal rutile structure to a non-magnetic semiconductor with monoclinic structure at $T = 340$ K [20]. Half of the orthorhombic distorted O_6-octahedra are filled with one V atom in the metallic high temperature phase. Despite decades of studies the nature of these phases in VO_2 is not fully understood. The mechanism of the MIT in VO_2 has been mainly ascribed to a crystallographic distortion and the resulting electron–phonon interaction [21], but electron correlation effects [19] may play an important role as well. Doping of VO_2 with electron donors (e.g. with Nb, Mo, W, Re or F) results in a linear decrease of the MIT temperatures proportional to the dopant concentration. Metallic monoclinic MoO_2 [22] is isostructural to the low temperature semiconducting phase of VO_2. By doping VO_2 with Mo the MIT temperature for the $Mo_xV_{1-x}O_2$ compound system is decreased [4]. Besides the industrial relevance of $Mo_xV_{1-x}O_2$ for thermochromic window coatings [23], the study of the nature of its MIT is also still of general interest and can reveal further details about the MIT also in undoped VO_2.

We investigated the room temperature electronic structure of these vanadium oxides by means of soft X-ray absorption spectroscopy (SXAS) and resonant soft X-ray emission spectroscopy (RSXES). In particular we discuss RSXE spectra of NaV_2O_5 and V_2O_3, presented by Schmitt et al. [34] in a more descriptive manner, and compare them with cluster model calculations that allow us to assign electronic transitions to their respective spectral contributions. SXAS is used as a means to determine the resonant excitation energies for the RSXES experiments. SXES is based on a two-photon process and it is known to reflect local partial density-of-states (LPDOS) for wide-band materials. Core electrons excited by X-ray photons undergo a transition to an intermediate core-excited state. This intermediate state decays to a final valence excited state or the ground state in a radiative process by emitting an X-ray photon. Since RSXES is a photon-in–photon-out technique in which excitations are registered as an energy loss with respect to the incoming photon energy, it is often called resonant inelastic X-ray scattering (RIXS) [24]. With RIXS we denote the part of the RSXE spectrum originating from low energy local electronic excitations (e.g. dd-excitations), which disperse linearly with the incoming photon energy, i.e. Raman scattering. Such excitations show up as energy loss peaks and an elastic peak at zero energy loss corresponds to a direct decay to the ground state. The parts of the RSXE spectra that do not behave as Raman scattering, and thus are stationary in X-ray emission energy, are denoted as ‘ordinary fluorescence’ [24]. This ordinary fluorescence part is related to the LPDOS of the material. Thus RSXE spectra generally consist of three ‘components’: ordinary fluorescence at fixed X-ray emission energy, RIXS contributions at constant energy loss and elastic scattering at the incoming photon energy. Local electronic excitations are often a consequence of electron correlation in 3d-transition metal compounds such as vanadates and give prominent RIXS contributions in L-edge RSXE spectra. In conventional optical absorption techniques transitions between states with the same angular momentum quantum number l are very weak due to the dipole selection rule. Therefore, dd excitations and in particular the correlation induced gap between V $3d_{xy}$ and V $3d^*_{xy}$ in NaV_2O_5 is difficult to study in optical absorption and RSXES is the method of choice for such cases. A more extensive description of the RSXE process [24] and its capability to study correlated materials such as vanadates and cuprates is given elsewhere in this volume [25].

2. Experimental

The investigated vanadium oxide samples were single crystals (approx. 2 mm × 2 mm × 0.1 mm) and all experiments were performed at room temperature. SXA and RSXES experiments were performed at the undulator beam lines 7.0.1 [26] at the Advanced Light Source (Lawrence Berkeley National Laboratory, USA) and I511-3 [27] at MAX II (MAX-lab National Laboratory, Lund University, Sweden). Beamline I511 comprises a modified SX-700 monochromator layout and beamline 7 is based on a spherical grating monochromator design. X-Ray absorption spectra were measured by recording the total electron yield (TEY) by measuring sample drain current while scanning the photon energy of the incident monochromatized synchrotron radiation. The SXA spectra were normalized to the photo current from a clean gold mesh introduced into the synchrotron radiation beam in order to correct for intensity variations of the incident X-ray beam. Soft X-ray fluorescence was recorded with a high-resolution Rowland-mount grazing-incidence grating spectrometer [28] with a two-dimensional detector. X-Ray photons were detected parallel to the polarization vector of the incoming

beam, which minimizes quasi-elastic scattering. For SXA spectra and excitation of RSXE spectra a monochromator energy band pass of 0.15 eV and 0.25 eV, respectively, was used. The total energy resolution (combined from excitation and spectrometer energy resolution) of the RSXE experiments was determined to be 0.6 eV by measuring the full-width-at-half-maximum (FWHM) at the elastic peaks.

The X-ray emission energy was calibrated by recording the characteristic Zn $L_{\alpha,\beta}$ spin–orbit doublet in 2nd order of diffraction, i.e. the $3d–2p_{3/2,1/2}$ transitions, from a clean Zn-foil and using the tabulated characteristic X-ray line energies from Bearden [29]. A common energy scale for SXE and SXA spectra was determined by determining the peak positions of the elastically scattered X-rays in the RSXE spectra.

At beam line I511-3 (MAX II) refocusing optics situated in front of the measurement chamber and focusing the beam down to a vertical beam size of below 20 μm is employed. This facilitates taking RSXE spectra without an entrance slit, i.e. the beam spot on the sample is the source for the soft X-ray emission spectrometer, and thereby achieving an energy resolution corresponding to a 15–20-μm entrance slit width and a considerable gain in solid angle of radiation reaching the detector. At beamline 7 a spectrometer entrance slit width of 15–20 μm had to be chosen in order to record high-resolution spectra with the same resolution.

3. Calculations

The experimental V 2p RSXE spectra presented in the next section are compared to model calculations. These calculations were performed in O_h symmetry with a single vanadium site VO_6 cluster model [30] in the framework of an Anderson impurity model [24]. For NaV_2O_5 the basic structural units consist of distorted VO_5 pyramids connected in the *a*–*b* plane to layers. These layers are stacked along the *c*-axis separated by Na^+ ions between them [6,15]. The distorted VO_5 pyramids were approximated by VO_6 clusters in order to simplify the calculation procedure. NaV_2O_5 is in a mixed valence state with a formal valence of $V^{4.5+}$ [6]. In order to account for these mixed valences the spectra were calculated for the V^{4+} (V $3d^1$) and V^{5+} (V $3d^0$) oxidation states independently and superimposed using the Kramers–Heisenberg formula [24,30]. For V_2O_3 only one spectrum for the corresponding V^{3+} (V $3d^2$) valence has to be calculated with the help of the Kramers–Heisenberg formula.

Experiments and calculations were carried out for emitted photons detected in a direction parallel to the polarization vector of the incident X-ray beam. This geometrical configuration minimizes the elastic contribution. Nevertheless, for both NaV_2O_5 and V_2O_3, an elastic peak appears in the RSXES experiments as well as in the cluster model calculations. This behavior can be explained by the group theoretical considerations described by Matsubara et al. [30].

Table 1
Adjustable parameters of the cluster model Hamiltonian for NaV_2O_5 and V_2O_3

	Δ (eV)	U_{dd} (eV)	U_{dc} (eV)	V (e_g) (eV)	$10Dq$ (eV)
NaV_2O_5, V^{4+}	4.0	4.0	4.8	3.1	0.7
NaV_2O_5, V^{5+}	0	4.0	4.8	3.1	0.7
V_2O_3, V^{3+}	6.0	4.5	5.3	2.9	1.4

For NaV_2O_5 the elastic peak originates from the V^{4+} ($3d^1$) component, whose ground state symmetry is T_{2g}. The V^{5+} (V $3d^0$) part with ground state symmetry A_{1g} does not contribute to elastic scattering. Moreover, V_2O_3 as a compound with V^{3+} (V $3d^2$) valence configuration shows an elastic peak due to its T_{1g} ground state symmetry.

The adjustable parameters of the Anderson impurity Hamiltonian for the V 2p RSXES model calculations for vanadium oxides are the charge transfer energy $\Delta = E(d_{n+1}\underline{L}) - E(d_n)$ between V 3d and ligand O 2p orbitals, the on-site d–d Coulomb interaction U_{dd}, the intra-atomic core hole potential U_{dc}, the hybridization strength $V(e_g) = -2V(t_{2g})$ and the magnitude of the crystal field splitting $10Dq = \varepsilon(e_g) - \varepsilon(t_{2g})$. These parameters for NaV_2O_5 and V_2O_3 are tabulated in Table 1. Further details about the theoretical calculations and the formulation of the chosen cluster model Hamiltonian are described elsewhere [30]. The calculated RSXE spectra are presented by a direct comparison with the experimental V 2p RSXE spectra in the next section.

4. Results and discussion

4.1. NaV_2O_5

In Fig. 1a the V L and O K SXA spectrum of NaV_2O_5 is displayed. Between 513 and 528 eV the V L-spectrum is split into a spin–orbit doublet. The absorption band from 513 to 521 eV is derived from the V $2p_{3/2} \rightarrow$ V 3d transition (V L_3) and the one from 521 to 528 eV from the V $2p_{1/2} \rightarrow$ V 3d transition (V L_2). Just above the V L_2-edge (528 eV) the double-peaked O K-spectrum is centered around 531 eV (528–534 eV) and is attributed to O 2p states hybridized with unoccupied crystal field split V 3d states. The structure around 542 eV originates from hybridization between O 2p states and V 4sp states.

Fig. 1b shows the RSXE spectra of NaV_2O_5 excited at the energies indicated by the arrows (a)–(n) in the SXA spectrum in Fig. 1a. The V L_α-band ($3d \rightarrow 2p_{3/2}$) and the V L_β-band ($3d \rightarrow 2p_{1/2}$) are situated around 510 and 518 eV, respectively. Above the V L-emission band region the O K_α-emission band is spread around 525 eV. The overlap of the V L_α-, V L_β- and O K_α-band is visualized with bars at the energy scale of the emission spectra in Fig. 1b. By resonant excitation we can tune the energy to the different absorption

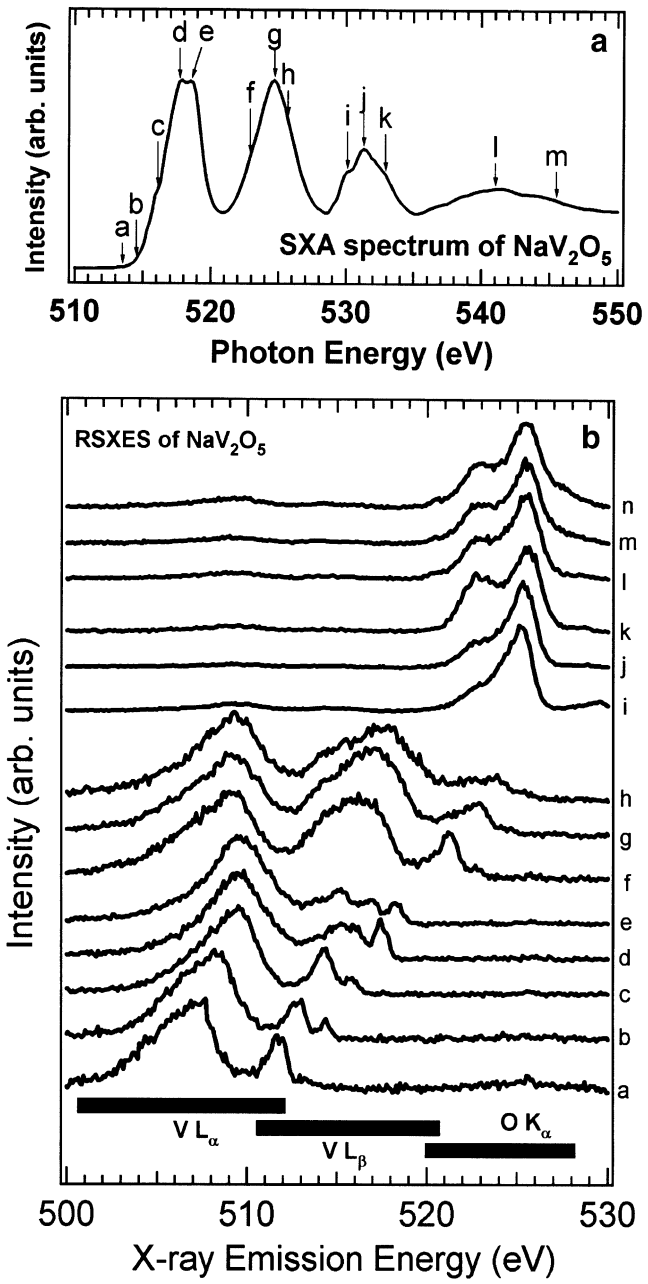

Fig. 1. (a) V L and O K soft X-ray absorption spectra of NaV_2O_5 in total electron yield mode. The excitation energies for the resonant soft X-ray emission spectra in (b) are marked through arrows above the spectrum. (b) Resonant soft X-ray emission spectra of NaV_2O_5 excited at the energies indicated by the arrows (a)–(n) in the absorption spectrum in (a) above. The energy regions of the overlapping V L_α-, V L_β- and O K_α-emission bands are marked through bars at the energy scale. The excitation energy dependence of these emission spectra visualizes that V L- and O K-emission spectra both consist of components originating from O 2p and V 3d bands, i.e. O 2p and V 3d electrons are strongly hybridized.

thresholds and thereby partially eliminate this overlap. Spectra (d) and (e) are dominated by the V L_α-emission band at approximately 510 eV in emission energy, which reflects the V 3d projected PDOS. In the RSXE spectra (f)–(h) besides the V L_α-emission band, the V L_β-emission band is also excited. Spectra (i)–(n) show the O K_α emission spectra and mainly display the O 2p projected PDOS. In all RSXE spectra ordinary V L-fluorescence is superimposed onto strong RIXS contributions. Only for the excitation energies above the O 2p threshold RIXS seems to be less pronounced.

A prominent feature in the resonantly excited spectra (a)–(h) at the V L thresholds disperses linearly with the elastic peak at an energy loss of approximately −1.6 eV. This loss structure is ascribed to a dd-excitation within the crystal field split 3d multiplet. Following this interpretation the dispersing band situated around 507 eV in X-ray emission energy in spectrum (a) cannot be interpreted as ordinary V L-fluorescence. Instead we interpret this as charge transfer (CT) states ($V3d^2\underline{L}$) showing up as RIXS features in our spectra. In Fig. 2 the RSXE spectra (a)–(h) are plotted against an energy loss scale relative to the elastic peaks and compared to the performed model calculations. This visual-

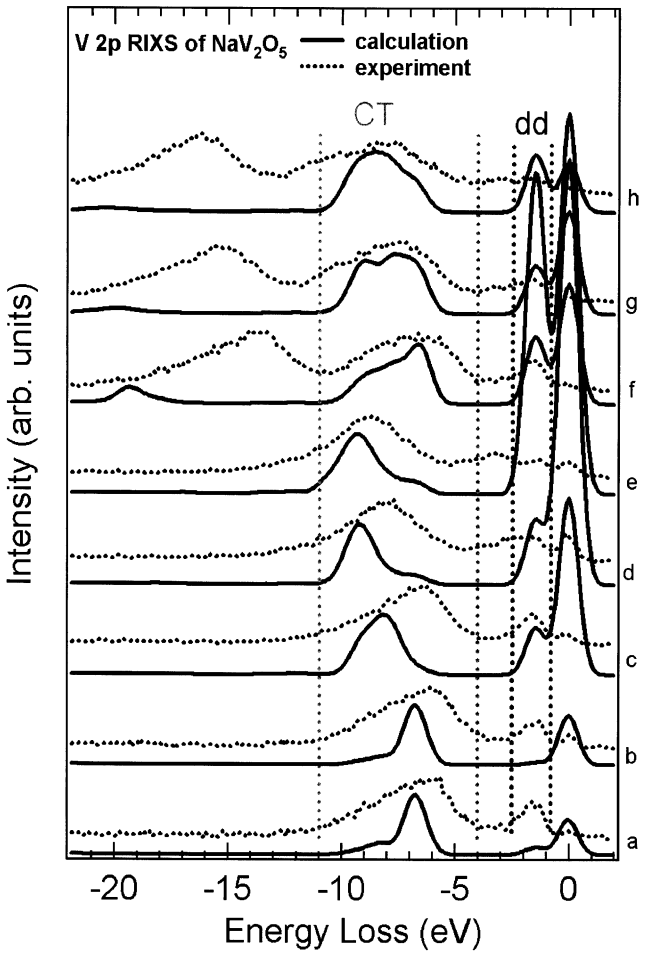

Fig. 2. Comparison of experiment and calculation of resonant soft X-ray emission spectra of NaV_2O_5 excited at V L-edge energies indicated by the arrows (a)–(h) in the absorption spectrum in Fig. 1a. The spectra are plotted against an energy loss scale relative to the elastic peaks. A peak at an energy loss of approximately −1.6 eV corresponding to a dd-excitation and a band of charge transfer states around −7 eV are marked through dashed lines.

izes that the model calculations give a good account for the dd-excitation peak, marked by dashed lines at a constant energy loss of −1.6 eV in the experimental spectra. According to the results from a recent LSDA + U band structure calculation [13] this energy loss feature can be attributed to a dd-excitation from the lower occupied Hubbard band Vd_{xy} to the upper unoccupied Hubbard band Vd^{*}_{xy}. In Wu and Zheng [13] the LSDA + U band structure calculations revealed a d–d transition gap of 0.6 eV. Our present RSXES investigation gives 1.6 eV, a much higher value for this correlation induced band gap and agrees well with a recent study by Zhang et al. [31] who observed a value of 1.56 ± 0.05 eV. In spectrum (a)–(c) of Fig. 2 a band situated around an energy loss of − 7 eV originating from CT states is marked by dashed lines.

Ordinary fluorescence contributions become increasingly significant for higher excitation energies. Spectra (a)–(c) consist mainly of RIXS contributions. Beginning with spectrum (d), which is excited at the maximum of the V L_3 absorption band, the CT band overlaps with the ordinary V L_α-fluorescence. In the same spectrum, a peak at lower energy adjacent to the dd-excitation peak appears and is ascribed to upcoming ordinary V L_β-fluorescence. Spectra (d)–(h) show a superposition of RIXS and ordinary fluorescence contributions and deviations between model and experiment are ascribed to this superposition. Ordinary fluorescence follows from delocalized intermediate states and cannot therefore be accounted for with our single vanadium site cluster model calculations [24,30]. Nevertheless, the position of the CT band is reproduced fairly accurately in the model calculations.

The good agreement of the experimental V 2p RIXS contribution in the RSXE spectra with the cluster model calculations corroborates the assumption of the highly correlated nature of NaV_2O_5. Furthermore, the ratio of inelastic scattering to ordinary fluorescence contributions gives a phenomenological measure of the localization in the intermediate core-hole state. From the dominance of the RIXS contributions in spectrum (a)–(c) we conclude that the states in the threshold region are strongly localized and indicative of a highly correlated material. The present cluster model calculations give a value of $U_{dd} = 4.0$ eV for the on-site d–d Coulomb energy, significantly higher than $U_{dd} = 3.0 \pm 0.2$ eV in Zhang et al. [31] who did not include oxygen orbitals and the intra-atomic core-hole potential into their model Hamiltonian.

Previously suggested dd-excitations at energies of 0.9–1.0 eV [8,10,11] are not observed in our RSXE spectra of NaV_2O_5. This may support the alternative interpretation of several authors [10,11] who attribute a bonding–antibonding transition within the V–O–V rung to the spectral feature seen in optical conductivity data at around 0.9–1.0 eV. Our observations and calculations also seem to exclude the possibility of a dd-excitation centered at an energy loss of 1.25 eV, at which energy a peak was observed in optical absorption [7] and assigned to a possible dd-excitation.

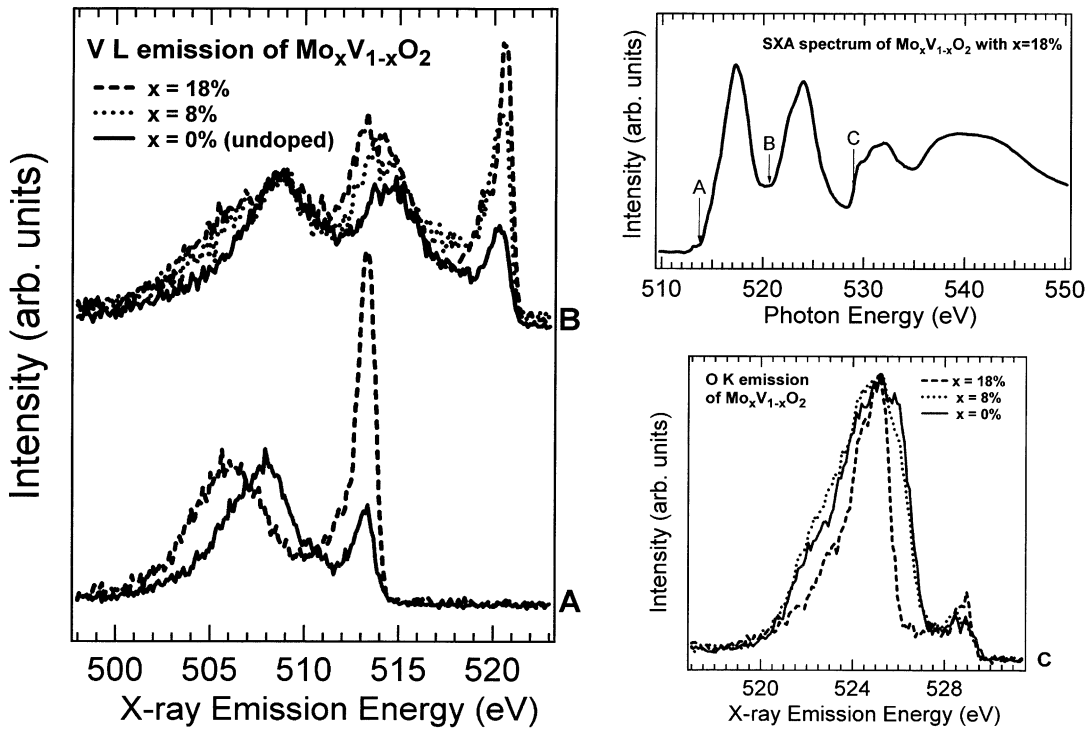

Fig. 3. Resonant soft X-ray emission spectra of $Mo_xV_{1-x}O_2$ with $x = 0$, 8 and 18% excited at the energies indicated by the arrows (A)–(C) in the absorption spectrum (upper right panel). O K emission (lower right panel) and V L emission (left panel) show drastic line shape and intensity changes for different doping content x. By doping with Mo, additional spectral features become visible and are associated with a successive filling of the V 3d-band.

4.2. $Mo_xV_{1-x}O_2$

By doping VO_2 with $x = 8\%$ and 18% Mo the MIT temperature of undoped VO_2, T_{MI} (0% Mo) = 340 K, is lowered to T_{MI} (8% Mo) = 225 K and T_{MI} (18% Mo) = 130 K, respectively. SXA spectra for Mo doped and undoped VO_2 [32] are similar, with respect to the positions of spectral features and the relative spectral intensities. Minor changes might be obscured by oxidation states present only at the surface of the single crystal samples. Especially, the employed TEY-mode is a relatively surface sensitive technique and therefore a much more bulk sensitive method seems to be advantageous for studying the subtle spectral changes for the different doping levels in Mo doped VO_2. RSXE spectroscopy is as a photon-in–photon-out technique such a method with bulk probing ability. As a test of the applicability of RSXE spectroscopy to study the Mo-doped VO_2 family, we compared RSXE spectra at V L- and O K-thresholds for two different doping levels with the undoped system.

Fig. 3 displays RSXE spectra of $Mo_xV_{1-x}O_2$ with $x = 0$, 8 and 18%. The corresponding excitation energies are indicated by the arrows (A)–(C) in the SXA spectrum of $Mo_xV_{1-x}O_2$ with $x = 18\%$ (upper right panel). O K emission (lower right panel) and V L emission (left panel) show dramatic changes of line shape and intensity for different doping content x. In the RSXE spectra of undoped VO_2 (solid line) RIXS structures seem to be rather weak, which favors a more bandlike interpretation of the electronic structure [19,21,33]. By doping with Mo, additional spectral features become visible.

A band around approximately 514 eV in X-ray emission energy, present in the spectra excited in between V L_3 and V L_2 absorption band labelled with (B) in Fig. 3, is associated mainly with V 3d PDOS [34,35]. We observed how spectral weight increases with Mo content x and related this to a filling of the V 3d band due to a corresponding increase of electron doping. Similar effects have recently been observed in a study of Li-ion intercalated vanadium oxide battery cathodes [36]. A double-peaked substructure splitting the V 3d band centered around approximately 514 eV might be indicative of additional RIXS features showing up in the RSXE spectra for increasing Mo doping content. The spectra excited at the pre-peak (A) display a rigid shift of the spectral weight originating predominantly from O 2p PDOS from approximately 508 to 506 eV in emitted photon energy upon doping VO_2 with 18% Mo. This spectral behavior is interpreted as a consequence of the V 3d band-filling and a quasi-rigid band behavior [22,33]. The spectral evolution of the O K-emission excited at the threshold (C) is extraordinary. Here the O K-emission spectrum for $x = 18\%$ is much narrower than for $x = 0$ and 8%. A possible explanation could be a change in the degree of O 2p–V 3d hybridization induced by the Mo doping; more detailed studies about this are in preparation [40].

4.3. V_2O_3

In Fig. 4 a comparison between V 2p RSXES experiments and calculations of V_2O_3 is displayed. The corresponding resonant excitation energies are marked by the arrows (D),

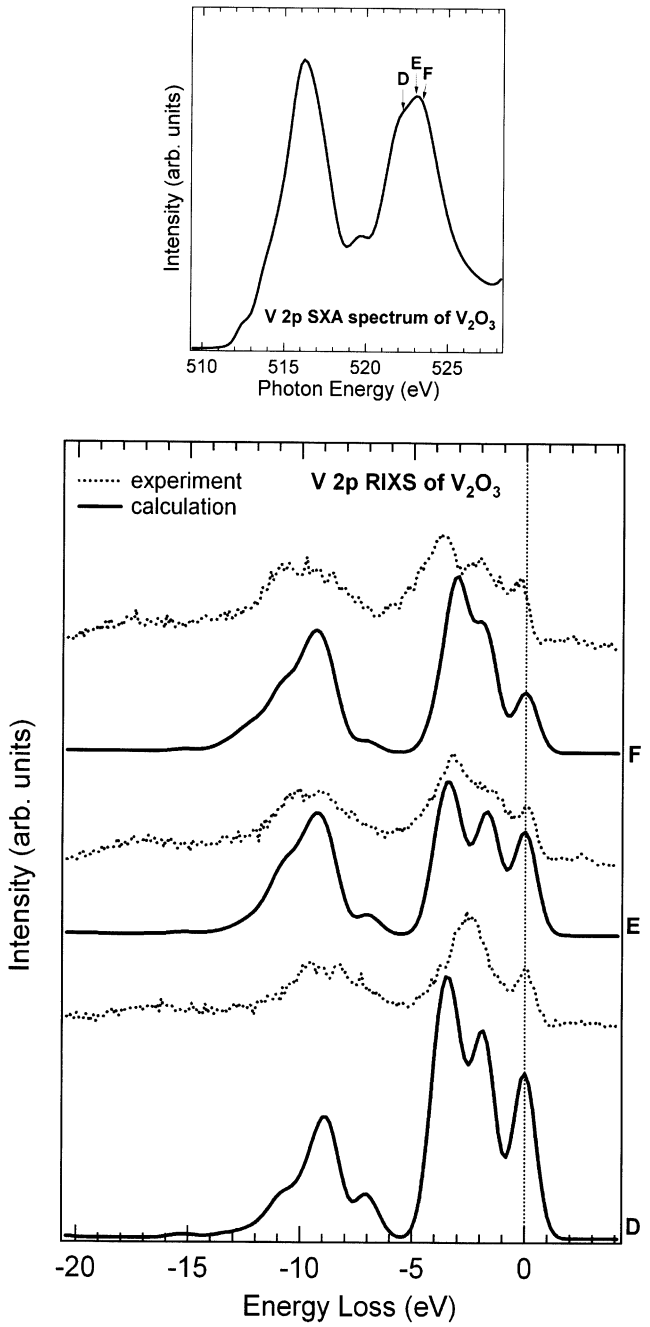

Fig. 4. V 2p RSXES experiments and calculations of V_2O_3. The elastic peak at 0 eV is marked by a dotted line. The excitation energies for the RSXE spectra are indicated by the arrows (D), (E) and (F) in the V 2p absorption spectrum above. A dd-excitation around −1.8 eV in photon energy loss is well accounted for by the calculation. Nevertheless, V 2p RIXS seems to be less prominent as in the case of NaV_2O_5. This can be attributed to a lower degree of correlation in V_2O_3 compared to NaV_2O_5. The spectra consist of an overlap between RIXS structures and ordinary fluorescence.

(E) and (F) in the V 2p absorption spectrum above the RSXE spectra. Here we present only V 2p RSXE spectra that show prominent inelastic contributions and are suitable for a comparison between experiment and theory. A more complete picture and discussion of RSXE spectra at V L and O K excitation energies has been already given by Schmitt et al. [34].

At −1.8 eV energy loss a dd-excitation is predicted by the model calculations and the experimental spectra show a corresponding structure at this energy loss. Such a dd-excitation was also discovered in a recent RSXES study of 1.5% Cr-doped V_2O_3 in the metallic state [37]. Another dd-excitation peak (at approx. −3.3 eV) and the CT-excitation band (between −7 and −12 eV) predicted by the model calculations are obscured by contributions from ordinary fluorescence that fall at the same photon energy. This is the V L_β-fluorescence (showing no excitation energy dependence [34]), which reflects the LPDOS and thereby reveals the band structure close to the Fermi level, where one part is interpreted as having a pure V 3d-character whereas the other part comes from V 3d states strongly hybridized with O 2p-states [34,38].

Interestingly, the prominent RIXS contributions of the present RSXES investigation of V_2O_3 show up at excitation energies far from the threshold in contrast to the case of NaV_2O_5. Moreover, V 2p RIXS at other energies is much less pronounced in V_2O_3 than in NaV_2O_5. This is attributed to the metallic character of V_2O_3 at room temperature and to a lower degree of electron correlation compared to NaV_2O_5. RIXS in metallic materials is assumed to be less pronounced since the amount of possible relaxation processes is much higher than for insulators having a band gap around the Fermi-level. Following the reasoning above, the RSXE spectra of V_2O_3 consist of an overlap between RIXS structures and ordinary fluorescence.

5. Summary and conclusions

V L- and O K-emission bands of vanadium oxides show considerable overlap. However, by using tunable excitation energies we can separate the respective V 3d and O 2p PDOS of the valence band by exciting RSXE spectra at the V L- and O K-absorption threshold, respectively. Strong hybridization between O 2p and V 3d electron bands [38] allows both the V L- and O K-emission spectra to consist of components originating from both bands. To our knowledge there is no closed theoretical formalism describing all RSXES contributions [24]. However, our studies suggest that the ratio of RIXS to ordinary fluorescence can be considered as a phenomenological measure for the degree of electron correlation and localization in the intermediate core-hole state at the chosen excitation energy. For NaV_2O_5, dd-excitations of −1.6 eV are observed together with charge transfer excitations of approximately −7 eV in photon energy loss. These dd-excitations, interpreted as transitions from the lower Hubbard band V $3d_{xy}$ to the upper Hubbard band V $3d^*_{xy}$, give a measure for the correlation induced band gap in this highly correlated Mott-insulator [31].

RIXS in V_2O_3 is considerably weaker, perhaps due to the metallic character at room temperature and a presumably lower degree of electron correlation. Nevertheless, energy loss features showing up in the RSXE spectra of V_2O_3 at −1.8 eV are attributed to dd-excitations within the crystal field split V 3d multiplet. We report drastic line shape changes in the RSXE spectra for different doping contents x of the $Mo_xV_{1-x}O_2$ system. These spectral changes are attributed to a successive filling of the V 3d band, that achieves more metallic character for increasing x.

A straightforward identification of different contributions in RSXES investigations of vanadium oxides is hampered by the superposition of RIXS and ordinary fluorescence. A way to quench the ordinary fluorescence channel might lie in employing excitation of spectra at the V 3p threshold. Generally M-fluorescence is much weaker than L-fluorescence for 3d-transition metals and therefore dd-excitations could be studied without being obscured by ordinary fluorescence contributions. Since 3p binding energies are approximately one-tenth of 2p binding energies, the absolute energy resolution is dramatically increased in such an experiment. Recently, experiments of this kind have been successfully performed at Cu 3p thresholds [25,39] and promise new insights in the correlated nature of the electronic structure also for vanadium oxides in the future.

Acknowledgements

We thank Dr M. Klemm, Prof. S. Horn (Institut für Physik, Universität Augsburg), G. Dhalenne and Prof. A. Revcoleschi (Laboratoire de Physico-Chimie de l'Etat Solide, Université de Paris-Sud) for providing us with the vanadium oxide samples for our investigations. This work was supported by the Swedish Research Council (VR) and the Göran Gustavsson Foundation for Research in Natural Sciences and Medicine. The experimental work was performed at the Advanced Light Source (ALS) and at MAX-lab. The ALS is supported by the Office of Basic Energy Sciences, Materials Science Division, of the US Department of Energy under Contract No. DE-AC03-76SF00098. We gratefully acknowledge G. Meigs (ALS) and C. Glover (MAX-lab) for excellent support and working conditions at beam line 7.0.1 (ALS) and I511 (MAX-lab).

References

[1] M. Imada, A. Fujimori, Y. Tokura, Rev. Mod. Phys. 70 (1998) 1039; N.F. Mott, Metal–Insulator Transitions, 2nd Edition, Taylor and Francis, 1990.
[2] M. Föex, C. R. Hebd. Sean. Acad. Sci. B 223 (1946) 1126.

[3] M. Marezio, D.B. McWhan, J.P. Remeika, P.D. Dernier, Phys. Rev. B 5 (1972) 2541;
F.J. Morin, Phys. Rev. Lett. 8 (1959) 34;
P.B. Allen, R.M. Wentzcovitch, W.W. Schulz, P.C. Canfield, Phys. Rev. B 48 (1993) 4359.
[4] T. Hörlin, T. Niklewski, M. Nygren, Mater. Res. Bull. 8 (1973) 179; M. Nygren, Chem. Commun. 11 (1973) 1.
[5] M. Isobe, Y. Ueda, J. Phys. Soc. Jpn. 65 (1996) 1178;
M. Lohmann, H.-A. Krug von Nidda, M.V. Eremin, A. Loidl, G. Obermeier, S. Horn, Phys. Rev. Lett. 85 (2000) 1742.
[6] H. Smolinski, C. Gros, W. Weber, U. Peuchert, G. Roth, M. Weiden, et al., Phys. Rev. Lett. 80 (1998) 5164.
[7] S.A. Golubchik, M. Isobe, A.N. Ivlev, B.N. Mavrin, M.N. Popova, A.B. Sushkov, et al., J. Phys. Soc. Jpn. 66 (1997) 4042.
[8] V.C. Long, Z. Zhu, J.L. Musfeldt, X. Wei, H.-J. Koo, M.-H. Whangbo, et al., Phys. Rev. B 60 (1999) 15721.
[9] A. Damascelli, C. Presura, D. van der Marel, J. Jegoudez, A. Revcolevschi, Phys. Rev. B 61 (2000) 2535.
[10] C. Presura, D. van der Marel, M. Dischner, C. Geibel, R.K. Kremer, Phys. Rev. B 62 (2000) 16522.
[11] M.J. Konstantinovic, J. Dong, M.E. Ziaei, B.P. Clayman, J.C. Irwin, K. Yakushi, et al., Phys. Rev. B 63 (2001) 121102(R).
[12] Z.S. Popovic, F.R. Vukajlovic, Phys. Rev. B 59 (1999) 5333.
[13] H. Wu, Q. Zheng, Phys. Rev. B 59 (1999) 15027.
[14] A.N. Yaresko, V.N. Antonov, H. Eschrig, P. Thalmeier, P. Fulde, Phys. Rev. B 62 (2000) 15538.
[15] S. Atzkern, M. Knupfer, M.S. Golden, J. Fink, A.N. Yaresko, V.N. Antonov, et al., Phys. Rev. B 63 (2001) 165113.
[16] R.M. Moon, Phys. Rev. Lett. 25 (1970) 527.
[17] P.D. Dernier, M. Marezio, Phys. Rev. B 2 (1970) 3771.
[18] C. Castellani, C.R. Natoli, J. Ranninger, Phys. Rev. B 18 (1978) 5001;
S.A. Carter, J. Yang, T.F. Rosenbaum, J. Spalek, J.M. Honig, Phys. Rev. B 43 (1991) 607;
G.A. Thomas, D.H. Rapkine, S.A. Carter, A.J. Millis, T.F. Rosenbaum, P. Metcalf, et al., Phys. Rev. Lett. 73 (1994) 1529.
[19] S. Shin, S. Suga, M. Taniguchi, M. Fujisawa, H. Kanzaki, A. Fujimori, et al., Phys. Rev. B 41 (1990) 4993.
[20] D.B. McWhan, M. Marezio, J.P. Remeika, P.D. Dernier, Phys. Rev. B 10 (1974) 490;
A. Zylbersztejn, N.F. Mott, Phys. Rev. B 11 (1975) 4383.
[21] M. Gupta, A.J. Freeman, D.E. Ellis, Phys. Rev. B 16 (1977) 3338; R.M. Wentzcovitch, J.L. Martins, G.D. Price, Phys. Rev. Lett. 72 (1994) 3389.
[22] V. Eyert, R. Horny, K.-H. Höck, S. Horn, J. Phys.: Condens. Matter 12 (2000) 4923, and references therein.
[23] T. Christman, B. Felde, W. Niessner, D. Schalch, A. Scharmann, Thin Solid Films 287 (1996) 134.
[24] A. Kotani, S. Shin, Rev. Mod. Phys. 73 (2001) 203.
[25] L.-C. Duda, T. Schmitt, A. Augustsson, J. Nordgren, J. Alloys Comp. 362 (2003) in press.
[26] T. Warwick, P. Heimann, D. Mossessian, W. McKinney, H. Padmore, Rev. Sci. Instrum. 66 (1995) 2037.
[27] R. Denecke, P. Väterlein, M. Bässler, N. Wassdahl, S. Butorin, A. Nilsson, et al., J. Electron Spectr. 101–103 (1999) 971.
[28] J. Nordgren, G. Bray, S. Cramm, R. Nyholm, J.-E. Rubensson, N. Wassdahl, Rev. Sci. Instrum. 66 (1989) 1690.
[29] J.A. Bearden, Rev. Mod. Phys. 39 (1967) 78.
[30] M. Matsubara, T. Uozumi, A. Kotani, Y. Harada, S. Shin, J. Phys. Soc. Jpn. 69 (2000) 1558;
M. Matsubara, T. Uozumi, A. Kotani, Y. Harada, S. Shin, J. Phys. Soc. Jpn. 71 (2002) 347.
[31] G.P. Zhang, T.A. Callcott, G.T. Woods, L. Lin, B. Sales, D. Mandrus, J. He, Phys. Rev. Lett. 88 (2002) 077401.
[32] M. Abbate, F.M.F. de Groot, J.C. Fuggle, Y.J. Ma, C.T. Chen, F. Sette, et al., Phys. Rev. B 43 (1991) 7263.
[33] E.Z. Kurmaev, V.M. Cherkashenko, Y.M. Yarmoshenko, S. Bartowski, A.V. Postnikov, M. Neumann, et al., J. Phys.: Condens. Matter 10 (1998) 4081.
[34] T. Schmitt, L.-C. Duda, A. Augustsson, J.-H. Guo, J. Nordgren, J.E. Downes, et al., Surf. Rev. Lett. 9 (2002) 1369.
[35] L.-C. Duda, C.B. Stagarescu, J.E. Downes, K.E. Smith, G. Dräger, Materials Research Society Symposium Proc.Vl. 494, Science and Technology of Magnetic Oxides.
[36] A. Augustsson, T. Schmitt, L.-C. Duda, J. Nordgren, S. Nordlinder, K. Edström, T. Gustafsson, J. Appl. Phys. (submitted).
[37] K.E. Smith, Solid State Sci. 4 (2002) 359.
[38] R. Zimmermann, R. Claessen, F. Reinert, P. Steiner, S. Hüfner, J. Phys.: Condens. Matter 10 (1998) 5697.
[39] P. Kuiper, J.-H. Guo, C. Såthe, L.-C. Duda, J. Nordgren, J.J.M. Pothuizen, et al., Phys. Rev. Lett. 80 (1998) 5204.
[40] T. Schmitt, L.-C. Duda, J. Nordgren et al. (in preparation).